ELSEVIER

Biophysical Chemistry 89 (2001) 145–162

Biophysical Chemistry

www.elsevier.nl/locate/bpc

Molecular dynamics simulations of urea and thermal-induced denaturation of S-peptide analogue

Zhiyong Zhang, Yongjin Zhu[1], Yunyu Shi*

Laboratory of Structural Biology, School of Life Science, University of Science and Technology of China (USTC), Hefei, Anhui 230026, PR China

Received 27 June 2000; received in revised form 17 October 2000; accepted 20 October 2000

Abstract

Molecular dynamics simulations of the S-peptide analogue AETAAAKFLREHMDS in water at 278 and 358 K, and in 8 M urea at 278 K were performed. The results show agreement with experiments. The helix is stable at low temperature (278 K), while at 358 K, unfolding is observed. The effects of urea on protein stability have been studied. The data support a model in which urea denatures proteins by: (1) diminishing the hydrophobic effect by displacing water molecules from the solvent shell around nonpolar groups; and (2) binding directly to amide units (NH and CO groups) via hydrogen bonds. The results of cluster analysis and essential dynamics analysis suggest that the mechanism of urea and thermal-induced denaturation may not be the same.

Keywords: Molecular dynamics; Denaturation; Hydrophobic effects; Hydrogen bonds; Cluster analysis; Essential dynamics analysis

1. Introduction

The details and mechanism of protein folding and unfolding are not completely understood now. In spite of the potential difficulties, great strides have been made in the experimental study of this problem. In order to enhance the rate of unfolding, some techniques have often been used in the experiments, such as high temperature, elevated pressure, low pH or chemical denaturants such as guanidinium chloride or urea.

Although it has been known for many years that adding urea to protein solutions can cause denaturation [1], the molecular mechanism of this effect is still not well understood. It is not clear if

* Corresponding author. Tel.: +86-551-3603754; fax: +86-551-3603754.

E-mail address: yyshi@ustc.edu.cn (Y. Shi).

[1] New address: 231 South, 34th Street, #7, Department of Chemistry, University of Pennsylvania, Philadelphia, PA 19104, USA.

0301-4622/01/$ - see front matter
PII: S0301-4622(00)00227-1

urea acts by directly binding to the protein, or indirectly through effects on the solvent [2–5]. Model studies on the solubility of hydrocarbons and peptides support either a bulk solvent effect by which the denaturants make water a 'more hydrophobic' medium or direct interactions between the denaturants and polypeptide, which favor the unfolded state [6]. Some experiments through surface tension [7] and calorimeter [8] support a mechanism involving direct interactions. An extensive kinetic study of the inhibition of ribonuclease A and papain by urea suggests that the effect of urea on activities of these enzymes can be well described by the denaturant binding model [9]. A study of a homologous series of cyclic dipeptides into aqueous urea solutions of varying concentrations at 298 K using calorimetery was performed [10]. The results support a model in which urea denatures proteins by decreasing the hydrophobic effects and by directly binding to amide units (NH and CO groups in the protein) via hydrogen bonds.

However, the mechanism of urea's effect at the molecular level is a rather difficult problem to address by experiments, since direct probes in a protein-denaturant-water system are lacking. MD (Molecular Dynamics) simulations could be effective in the interpretation of the experimental results and the understanding of the urea-induced denaturation of proteins. MD simulations of the unfolding of barnase in 8 M aqueous urea were performed [11,12]. Tirado-Rives' results [11] suggest a plausible model for the effect of urea in protein denaturation: urea molecules accumulate in excess near the protein surface and form hydrogen bonds with the polar groups; the displacement of water molecules from the first shell leads to greater exposure of nonpolar side chains. The urea molecules also act both as a scaffold for the remaining water molecules, further minimizing their contact with the hydrophobic groups, and as a wedge to separate groups previously forming intramolecular hydrogen bonds. Caflisch's results [12] indicate that an aqueous urea solution solvates the surface of a polypeptide chain more favorably than pure water. Urea molecules interact more favorably with nonpolar groups of the protein than water does, and the presence of urea improves the interactions of water molecules with the hydrophilic groups of the protein, that is, the urea denaturation involves effects on both nonpolar and polar groups of proteins.

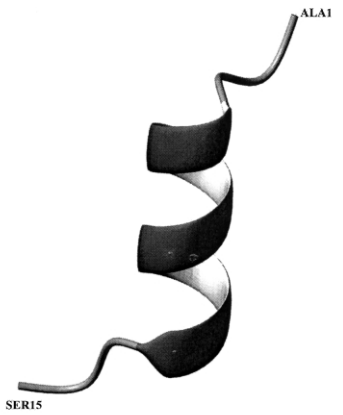


```
S-peptide: K-E-T-A-A-A-K-F-E-R-Q-H-M-D-S-S-T-S-A
           |                 |   |
  Analog:  A-E-T-A-A-A-K-F-L-R-E-H-M-D-S
```

Fig. 1. Initial structure of the S-peptide analogue and comparison of the sequences between the analogue and the native S-peptide. Residues in α-helix and the differences between the two sequences are shown. The figure was created using the program MOLMOL.

In this paper, MD simulations were undertaken to study the urea and thermal-induced unfolding of a α-helical analogue of Ribonuclease A S-peptide [13] with explicit solvent. S-peptide, isolated by subtilisin cleavage of the first 19–20 residues of Ribonuclease A, is approximately 30% helical at 273 K [14]. The 15-residue analogue of S-peptide was chosen amongst the many sequence variants of the S-peptide, the sequence of this peptide is compared to the native S-peptide as seen in Fig. 1.

This analogue has several advantages for the theoretical study of unfolding. Experimental data are available for comparison and reveal that at low temperature (278 K) the helix is stable, while unfolding is observed at 358 K. Compared with barnase (110 residues and $M_r = 12383$), the analogue has only 15 residues ($M_r = 1679$), so a much

longer MD simulation could be performed. The mode of action of urea molecules with protein and water molecules can be analyzed in more detail in order to provide insights on the mechanism of urea-induced denaturation at a molecular level.

A brief outline of this paper is as follows; in materials and methods, the tools used to perform MD simulations and to analysis are described. In results and discussion, simulations at different conditions are described. Here, we show the results of structural analysis on the equilibrium conformations in the different simulations. Subsequently, the action of urea molecules is discussed through hydrophobic contributions and hydrogen bonding interactions, respectively. We also compare urea and thermal-induced denaturation via cluster analysis and essential dynamics analysis. Finally, conclusions from this work are discussed.

2. Materials and methods

2.1. Molecular dynamics simulations

The initial coordinates were obtained from the X-ray structure of Ribonuclease S (PDB entry 1RNS) [15]. The first 15 residues were extracted. With only minor modifications (1 Lys/Ala, 9 Glu/Leu, 11 Gln/Glu, see Fig. 1), a good starting structure for our simulations was obtained. The peptide was protonated to give a zwitterionic form (with N-terminal $NH3^+$ and C-terminal COO^- groups), the negatively charged residues are Glu2 (−1), Glu11 (−1), Asp14 (−1) and the positively charged residues are Lys7 (+1), Arg10 (+1), His12 (+1), so the peptide gives a total charge of zero.

For the simulations in pure water, an empty cubic box was created first and the peptide was centered in the box (distance between the solute and the box is 0.8 nm), so the box size is 4.131 nm × 4.131 nm × 4.131 nm. Next, the peptide was solvated by stacking equilibrated boxes of water molecules. All water molecules were removed from the box where the distance between any atom of the solute molecule and any atom of the water molecules was less than the sum of the Van der Waals radii of both atoms. The resulting system was composed of the peptide and 2114 water molecules subjected to periodic boundary conditions. The system was subsequently energy minimized with a steepest decent method until the maximum force of the system is smaller than 100 kJ mol^{-1} nm^{-1}.

The simulation in 8 M urea was started from the same initial coordinates by first creating an empty cubic box of the same size, then 340 urea molecules were inserted in the box at random positions. Next the peptide was solvated by water molecules. The final system contained the peptide, 340 urea molecules and 1492 water molecules in a cubic box of dimensions 4.131 nm × 4.131 nm × 4.131 nm corresponding to approximately an 8 M urea concentration and a density of 1.151 g cm^{-3}. An energy minimization was performed with a steepest descent method until the maximum force of the system was smaller than 100 kJ mol^{-1} nm^{-1}.

To compare the dynamical behavior of the peptide at different temperatures, the simulations in pure water were carried out at 278 (CW) and 358 K (HW), respectively. The simulation in 8 M urea was performed at 278 K (CU) only.

All the MD simulations were performed using an isothermal-isobaric simulation algorithm [16]. The temperature was kept constant to a reference value by weak coupling to an external temperature bath. The time constant for coupling is 0.1 ps. The pressure was also kept constant by weak coupling to a bath of constant pressure ($P_0 = 1$ bar, coupling time $\tau_p = 1$ ps) [16]. The default GROMACS force field was used which is based on GROMOS-87 [17] with a small modification concerning the interaction between water-oxygen and carbon atoms, as well as 10 extra atom types [18]. For the water molecules, the SPC/E water model was used [19]. The LINCS algorithm was used to constrain all bond lengths [20]. The cutoff radius was set to 1.0 nm for Van der Waals interactions and 1.4 nm for Coulomb interactions, and the dielectric permittivity was set to 1. A time step of 2 fs was used. All simulations were equilibrated by 50 ps of MD with position restraints on the peptide to allow relaxation of the solvent molecules and all atoms were given an initial

velocity obtained from a Maxwellian distribution at the desired temperature. After which 20 ns data generation runs were performed for CW, CU and HW, respectively.

All MD runs and the trajectory analysis were performed using the GROMACS 2.0 software package [21]. DSSP was used to definite secondary structure [22].

2.2. Contact analysis

Contact analysis can compute the interactions between one group and a number of other groups in the simulated system. Considering one atom in a group of solvent molecules (urea or water), if the distance between this atom and any atom in the solution group was less than a given cutoff distance, a contact was defined. Considering every atom in the solvent group, we can calculate the total number of contacts between solvent and solution. Here, we selected a cutoff distance as 0.6 nm.

2.3. Cluster analysis

Cluster analysis is used to follow the distributions of diverse conformations along the folding-unfolding pathway. There are several different methods that can cluster structures. We use an algorithm (Zhu J, personal communication) similar to that used in DycoBlock (dynamical combination of molecular building blocks at binding site) [23]. For each pair of structures a least-square translational and rotational fit was performed using the backbone atoms of residues 4–8, and the atom-positional root-mean-square difference (RMSD) for this set of atoms was calculated. The RMSD cutoff for two structures to be considered similar was set to 0.1 nm. A structure was added to a cluster when the RMSD between this structure and the central structure of the cluster was less than the cutoff. Furthermore, if the internal energy of the structure was less than that of the central structure of the cluster, the newly added structure will become the new central structure of this cluster. In this way, the number of members in a cluster and the central structure of the cluster were both updated dynamically.

2.4. Essential dynamics

Essential dynamics analysis can distinguish large, concerted internal motion from small, random internal motion [24]. In short, this method comprises: (1) eliminating the overall translational and rotational motion because these are irrelevant for the internal motion; (2) constructing the atomic positional fluctuation covariance matrix $c_{ij} = \langle (x_i - \langle x_i \rangle)(x_j - \langle x_j \rangle) \rangle$, where x_i and x_j represent all Cartesian coordinates of the atoms we selected; (3) diagonalizing the symmetric matrix; and (4) sorting eigenvectors in order of decreasing value. Only motion along the first few eigenvectors describe significant motion in the protein, further eigenvectors often correspond to small Gaussian-distributed random fluctuations [24]. In this paper, we defined 'essential subspace' as motions that were characterized by a correlation coefficient less than 0.9 between the actually sampled distribution of a vector, with the Gaussian distribution calculated from its eigenvalue [25]. An estimate of inner products of eigenvector sets of different simulations can provide a valid method to assess their dynamical similarity [26]. Since the eigenvectors are normalized, an inner product of one means that eigenvectors are identical. To have a closer look at the motion along some eigenvector directions, one can project the trajectory onto these individual eigenvectors.

3. Results and discussion

3.1. Native structure

In Fig. 1 the initial structure of the peptide is shown. Residues 4–12 are in a α-helix conformation. The N-terminal residues 1–3 and the C-terminal residues 13–15, are random coils. There are five native hydrogen bonds; Phe8:NH-Ala4:CO, Leu9:NH-Ala5:CO, Arg10:NH-Ala6:CO, Glu11:NH-Lys7:CO and His12:NH-Phe:CO. There are seven hydrophobic residues (Ala1, Ala4, Ala5, Ala6, Phe8, Leu9 and Met13) and eight hydrophilic residues (Glu2, Thr3, Lys7, Arg10, Glu11, His12, Asp14 and Ser15).

3.2. Global behavior

DSSP algorithm is based on hydrogen-bonding patterns and geometrical features to determine the secondary structure [22]. In Fig. 2a the secondary structures are reported for the three simulations. During the 20 ns simulation in CW, the helix is relatively stable (residues 4–8), with only a minor unfold and refold several times of the helical structures. This shows agreement with experimental observations in that at low temperature, the peptide has a considerable population of the helical form in water. The higher stability of the helix near the N-terminus is consistent with Tirado-Rives' result [13]. This shows agreement with the higher helical propensity of the residues involved near the N-terminus (most notably the Ala4, Ala5 and Ala6 triad) [27,28]. In CU, the α-helix turns into a 5-helix (usually called π-helix) rapidly, and during the remaining time, the 5-helix is the major secondary-structural element. It seems that the 5-helix is an intermediate during the urea-induced unfolding process. In HW, the residues rapidly lose their native conformations after 6 ns which is also in good agreement with the experiments in that the peptide unfolding is observed at 358 K. But here, there is a difference between our result and Tirado-Rives' [13]. They performed 500 ps MD simulations of this peptide at 358 K and found that breaking of hydrogen bonds in pure water occurs through 3_{10}-helical conformations, whereas our result reports a conversion to a 5-helix. This difference may be a result of using different force field. (Tirado-Rives used Amber force field, whereas we used a Gromos-87 force field.)

The atom-positional root-mean-square deviations (RMSD) of the backbone atoms of residues 4–8 from the initial structure (Fig. 2b) was calculated for the three simulations. All RMSD in CW are less than 0.1 nm, which also indicates that the helix of residues 4–8 is stable. The RMSD of CU support our idea that the 5-helix is a relatively stable intermediate during the unfolding process. Since urea-induced denaturation is milder than thermal-induced denaturation, a complete unfolding of the peptide could not be observed during the 20 ns simulation time. From the RMSD of HW, we can see clearly the process from the folded structure, to the intermediate and finally to the completely unfolded state.

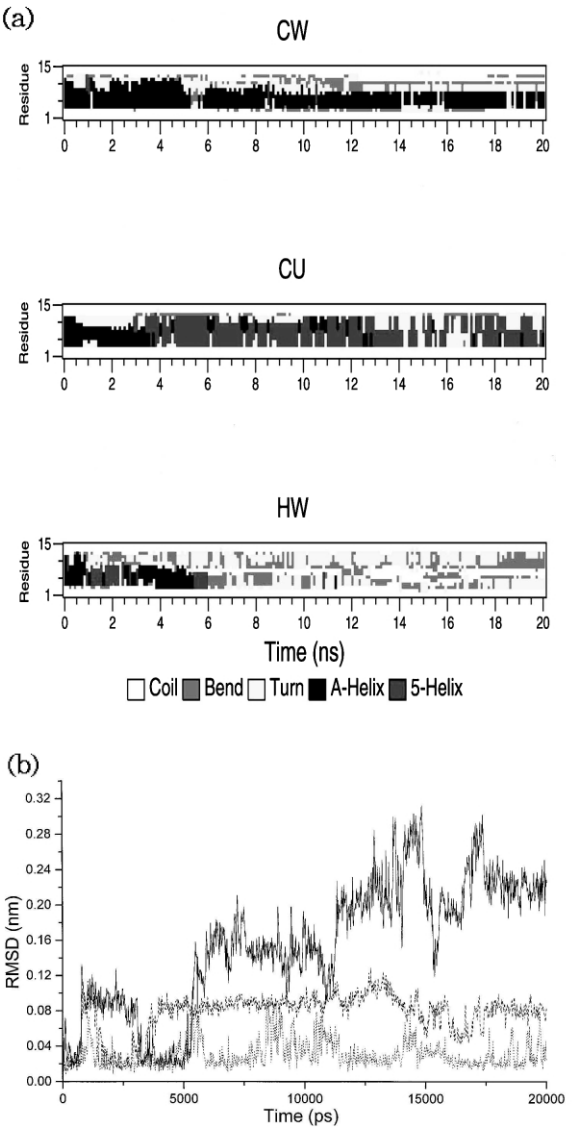

Fig. 2. (a) Secondary structures during simulations of CW, CU and HW. The assignments were made with the DSSP program [22]. (b) The atom-positional root-mean-square deviations (RMSD) of the backbone atoms of residues 4 to 8 from the initial structures. Dot: CW, dash: CU and solid: HW.

3.3. The mode of action of urea

3.3.1. Hydrophobic contributions

Tirado-Rives reported that the simulations in urea have noticeably more solvent-exposed hydrophobic areas than their aqueous counterparts, indicating that urea stabilizes hydrophobic residues that become exposed to solvent upon unfolding [11].

The solvent-accessible surface area (SASA, represented by the number of water molecules in contact with residues) of 4 hydrophobic residues (4,5,6 and 8) is shown (Fig. 3). According to our results, it is hard to say that 'the simulation in urea solution has a noticeably more solvent-exposed hydrophobic area' [11]. Instead, we can say that the solvent-exposed hydrophobic area in CU is much more stable than that in CW. In fact, in Tirado-Rives' article [11], the average solvent-accessible hydrophobic area of barnase over the last 100 ps of CW ($T = 298$ K) is 14.93 nm^2 and this value of CU ($T = 298$ K) is 15.16 nm^2. These two values are essentially the same, which is similar with Caflisch's [12] and our results. Noticeably more solvent-exposed hydrophobic area in urea solution than that in pure water is only observed at high temperature (358 K) in Tirado-Rives' results [11].

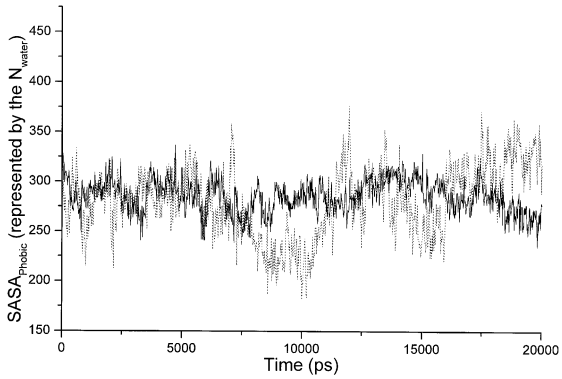

Fig. 3. The solvent-accessible surface area (SASA) of four hydrophobic residues of the residues 4–8 (represented by the number of water molecules in contact with the residues). Dot: CW; solid: CU.

We performed contact analysis (see Section 2) between nonpolar groups of the peptide and urea or water molecules (Fig. 4) in the solvation shell (cutoff = 0.6 nm) during the simulation of CW and CU. In CU, although the number of urea

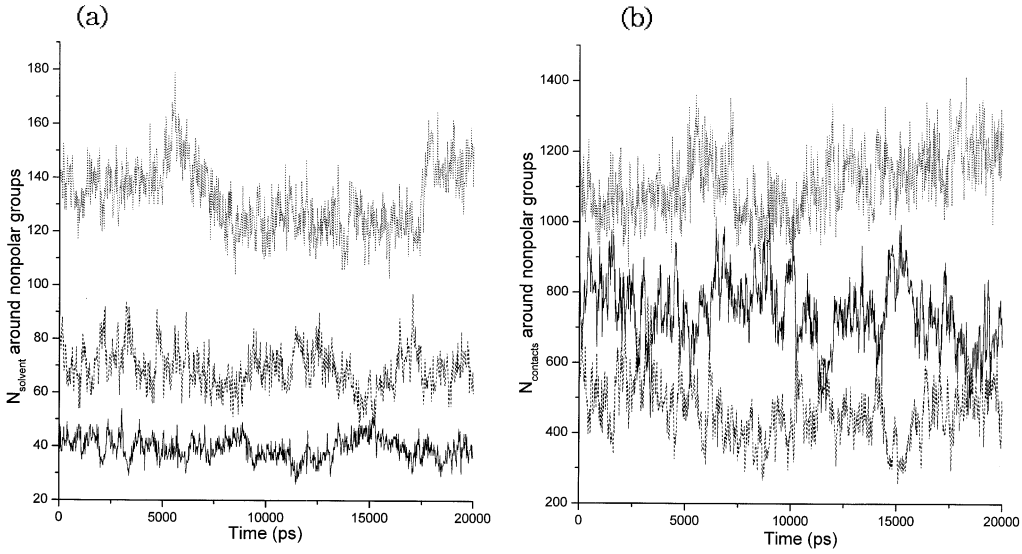

Fig. 4. Contact analysis (cutoff = 0.6 nm). (a) Number of urea or water molecules in contact with nonpolar groups on the peptide. (b) Number of contacts of urea or water molecules with nonpolar groups on the peptide. Dot: water (CW); dash: water (CU); solid: urea (CU).

molecules in the solvation shell is less than that of water molecules (Fig. 4a), the number of contacts between nonpolar groups of the peptide and urea is more than that between nonpolar groups and water (Fig. 4b). Our results show good agreement with Caflisch's in that urea molecules interact more favorably with nonpolar groups of the protein than water does [12].

But here, there is a question. Since the polarity of urea is stronger than water, the nonpolar interaction with aqueous urea should be enthalpically unfavorable. Why do urea molecules interact more favorably with nonpolar groups than water does?

Qin Zou et al. have determined the energetics of dissolution of a homologous series of cyclic dipeptides into aqueous urea solutions of varying concentrations at 298 K using a calorimeter [10]. The nonpolar transfer is characterized by a positive ΔH and a positive ΔS, indicating that the nonpolar interaction with aqueous urea is indeed enthalpically unfavorable but entropically favorable. That is, the favorable interaction of hydrophobic groups to urea solution arises from a favorable entropy change, which may suggest that urea decreases the hydrophobic effects.

But how does urea do this? It is well known that water is a very poor solvent for nonpolar molecules. The first step of the solvation of nonpolar molecules in water may be regarded as the formation of a cavity in the water into which the solute will fit [29]. The free energy required for the formation of such a cavity in liquid water will be large because it requires the separation of strongly interacting water molecules. Once a cavity is formed and the solute placed in it, the solvent will undergo any further changes that reduce the free energy of the system. With a polar solute, hydrogen bonds and other electrostatic interactions will occur between the solute and the water. These favorable interactions will compensate for the initial energy required for forming the cavity. However, a nonpolar solute will gain only the minor Van der Waals forces with the solvent. To compensate for the absence of favorable hydrogen bonds and electrostatic interactions with the solute, the solvent surrounding it will rearrange to form the most extensive number of hydrogen bonds between the water molecules. That is to say, the degree of ordering of water molecules around a nonpolar solute is more than in the case of the bulk region of water. When the nonpolar groups of the protein aggregate, some water molecules around them will be released and these released waters will regain the entropy. This effect may be regarded as the driving force of the hydrophobic interactions.

Considering the transfer of the nonpolar groups from water to urea. As urea is a larger molecule than water, it is able to displace several water molecules from around nonpolar groups (Fig. 4a). These displaced waters regain the entropy normally associated with hydrophobic hydration and thus, the transfer of hydrophobic groups from water to urea solution is accompanied by an increase in entropy. In urea solution, there are two differences in the solvation shell compared to the case of pure water: (1) the number of solvent molecules (urea and water) is much less (Fig. 4a); and (2) the degree of ordering of the solvent molecules around nonpolar groups may be less. These two effects can lead to a decrease of the hydrophobic interactions.

In conclusion, our data support the model that the hydrophobic contribution of urea's action is simply the result of its ability to displace water in the solvation shell [30–32]. If only considering the hydrophobic contributions, urea promotes protein unfolding through the stabilization of the unfolded or partly unfolded form rather than destabilizing the native state [11]. Our results of RMSD and the SASA support this idea.

3.3.2. Hydrogen-bonding interactions

Qin Zou et al. reported that the transfer of the amide unit (NHCO) from water to urea is characterized by a negative ΔH and a negative ΔS, indicating that the amide interaction with aqueous urea is enthalpically favorable and entropically unfavorable [10]. This result suggests that the amide-urea interaction is a specific interaction, most likely mediated through hydrogen-bonding interactions.

We monitored the first shell (cutoff = 0.35 nm) urea/water ratio during the simulation of CU. Although the urea/water ratio of the simulated

system is 0.228 (340/1492), this value in the first shell is much higher, and occasionally above 1.0 (Fig. 5a). This result indicates that the first shell contains more urea molecules than the bulk region, although the initial distribution was essentially uniform.

From Fig. 5b, we can see an obvious competition between urea-peptide and water-peptide hydrogen bonds. Although the number of urea molecules in the first shell is usually less than water, urea can form more hydrogen bonds than water does.

Table 1 lists the number of urea and water molecules in the first shell during each 1 ns simulation and in which the number of urea and water molecules that can form hydrogen bonds with the peptide for the three simulations. In the simulation of CU, approximately 72% of the urea molecules in the first shell (average of the 20 values, see Table 1) are involved in hydrogen bonds with the peptide, and approximately 60% of the first shell water molecules participate in hydrogen bonds with the peptide. While in CW, this percentage is approximately 77%. Our results indicate that the percentage of the urea molecules in the first shell, which are involved in hydrogen bonds with the peptide, is larger than that of water molecules. Urea molecules can form hydrogen bonds with the peptide more favorably (Table 1 and Fig. 6a). The number of water molecules in the first shell, which can form hydrogen bonds with the peptide in CU, is decreased compared with that in the CW (Table 1 and Fig. 6b) because of the existence of urea molecules in the former.

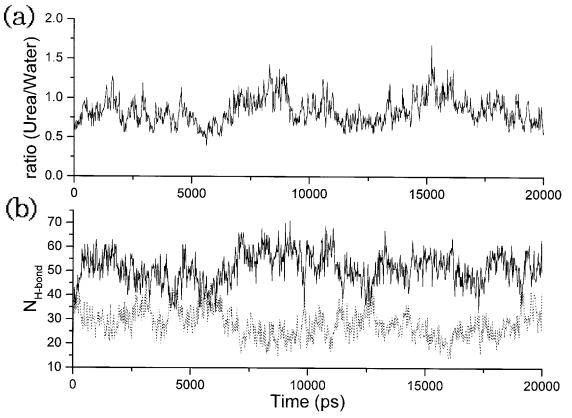

Fig. 5. (a) Ratio of urea/water in the first shell (cutoff = 0.35 nm) as a function of time during the simulation of CU. (b) Number of hydrogen bonds formed between urea or water molecules and the peptide as a function of time during the simulation of CU. Dot: water-peptide hydrogen bonds; and solid: urea-peptide hydrogen bonds.

Now, one question naturally arises as to how hydrogen-bonding interactions between urea and the peptide promote unfolding. Since most of the hydrogen bonds are between urea molecules and amide units (NHCO), a reasonable hypothesis is that the urea-amide hydrogen bonds affect the native hydrogen bonds of the protein.

Considering the five native hydrogen bonds in the initial structure of the peptide (Phe8:NH-Ala4:CO, Leu9:NH-Ala5:CO, Arg10:NH-Ala6:CO, Glu11:NH-Lys7:CO, and His12:NH-Phe8:CO). The distances between the NH and the CO, which are involved in these five hydrogen bonds, are computed, respectively, for all three simulations (Fig. 7, Arg10:NH-Ala6:CO). The details of hydrogen-bonding interactions between water or urea molecules and the amide units of residues 4–12 are analyzed (Table 2, Arg10).

There are some conclusions, which can be made from these results. (1) Urea-induced denaturation at low temperature is much milder than thermal-induced denaturation. (2) Hydrogen bonds of water molecules with the peptide are not stable enough to process peptide unfolding. (3) For urea molecules, the amount of hydrogen bonds between CO (urea) and NH (AA: amino acid), is less than that of hydrogen bonds between NH (urea) and CO (AA). Since the size of the urea molecule is larger than water, there exist a steric hindrance, which makes that the formation of CO (urea)-NH (AA) hydrogen bonds much more difficult than the formation of NH (urea)-CO (AA) hydrogen bonds. (4) It should be noted that there exist some very stable (long residence time) hydrogen bonds of CO (urea) with NH (AA) — Table 2, Arg10: 13,14,15,19,20 ns, the increased distance between NH (Arg10) and CO (Ala6) corresponds to these stable hydrogen bonds (Fig. 7). These results suggest that only stable hydrogen bonds between urea molecules and the peptide can facilitate peptide unfolding.

Table 1
The number of solvent molecules in the first shell of the peptide (cutoff = 0.35 nm) and within which, the number of solvent molecules which can form hydrogen bonds with the peptide for different simulations

ST (ns)[b]	Number of solvent molecules ($N_{\text{H-bond}}/N_{\text{in 0.35-nm}}$%)[a]							
	(CW Waters)		(CU Waters)		(CU Urea)		HW Waters	
	$N_{\text{in 0.35 nm}}$[c]	$N_{\text{H-bond}}$[d]	$N_{\text{in 0.35 nm}}$	$N_{\text{H-bond}}$	$N_{\text{in 0.35 nm}}$	$N_{\text{H-bond}}$	$N_{\text{in 0.35 nm}}$	$N_{\text{H-bond}}$
1	1655	1261 (76%)[e]	651	371 (57%)	144	92 (64%)	2048	1829 (89%)
2	1656	1250 (75%)	594	319 (54%)	146	102 (70%)	2033	1774 (87%)
3	1650	1287 (78%)	613	360 (59%)	145	100 (69%)	2017	1755 (87%)
4	1636	1222 (75%)	623	363 (58%)	139	98 (71%)	1995	1695 (85%)
5	1667	1273 (76%)	575	367 (64%)	141	107 (76%)	2016	1730 (86%)
6	1674	1271 (76%)	623	396 (64%)	131	99 (76%)	2011	1771 (88%)
7	1651	1299 (79%)	646	416 (64%)	133	94 (71%)	2005	1757 (88%)
8	1622	1251 (77%)	555	322 (58%)	144	100 (69%)	2005	1757 (88%)
9	1641	1257 (77%)	568	315 (55%)	149	119 (80%)	2011	1782 (87%)
10	1644	1288 (78%)	639	369 (58%)	136	95 (70%)	1990	1754 (88%)
11	1635	1261 (77%)	575	338 (59%)	132	91 (69%)	2013	1766 (88%)
12	1631	1230 (75%)	587	356 (61%)	135	102 (76%)	2026	1793 (88%)
13	1676	1264 (75%)	629	370 (59%)	126	100 (79%)	2023	1808 (89%)
14	1674	1295 (77%)	620	371 (60%)	135	91 (67%)	2051	1846 (90%)
15	1661	1272 (77%)	565	342 (61%)	141	96 (68%)	2026	1811 (89%)
16	1673	1289 (77%)	548	308 (56%)	131	100 (76%)	2023	1806 (89%)
17	1646	1250 (76%)	573	314 (55%)	142	97 (68%)	2022	1800 (89%)
18	1701	1314 (77%)	527	317 (60%)	142	104 (73%)	2033	1811 (89%)
19	1668	1299 (78%)	530	328 (62%)	146	108 (74%)	2048	1794 (88%)
20	1681	1294 (77%)	613	409 (67%)	154	120 (78%)	2015	1761 (87%)

[a] A maximal distance of 0.35 nm between donor and acceptor and a maximal angle of 60° between hydrogen-donor-acceptor were used.
[b] The analyses are performed over 1 ns each.
[c] The number of solvent molecules in the first shell.
[d] The number of solvent molecules that can form hydrogen bonds with the peptide in the first shell.
[e] The percentages of $N_{\text{H-bond}}/N_{\text{in 0.35-nm}}$ are in parentheses.

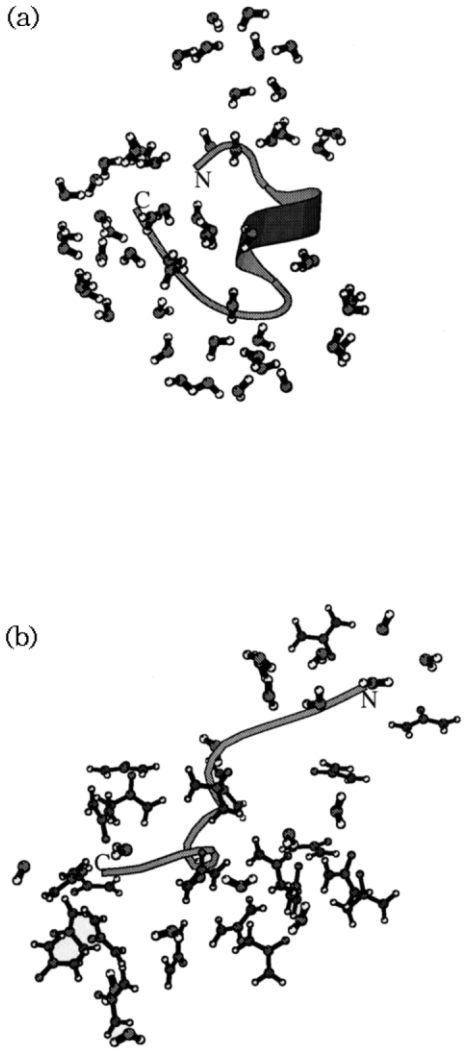

Fig. 6. Ribbon representations of the S-peptide analogue with solvent molecules (urea and water) that can form hydrogen bonds with the peptide. (a) CW ($t = 16495$ ps). (b) ($t = 16495$ ps). The figures are created using the program Molscript [39].

Why are these hydrogen bonds so stable? Robinson and Jencks proposed that the direct interaction of urea with polar groups of the protein via multiple hydrogen bonds is responsible for the 'nonhydrophobic' effect of the chemical denaturants of the urea-guanidinium class [33]. Further analysis reveal that these stable hydrogen bonds in our simulation of CU form between 94Urea (CO), 113Urea (CO) and Arg10 (NH). We computed all hydrogen bonds of 94Urea and 113Urea, with polar groups on the peptide in order to see if 94Urea and 113Urea can form multiple hydrogen bonds with the peptide. Our results indicate the existence of multiple hydrogen bonds between urea and the peptide (Table 3), which have obvious effects on the native hydrogen bonds. In our simulation, two forms of multiple hydrogen bonds are observed (Table 3), in agreement with Robinson and Jencks [33] (Fig. 8).

In summary, the analysis of the interactions between urea molecules and amide units suggests that the 'nonhydrophobic' effects of urea-induced denaturation is a result of urea's ability to break hydrogen bonds in the peptide via stable, multiple hydrogen bonds between urea molecules and amide units.

There are two main thermodynamic models that are used to analyze urea-induced protein denaturation curves [3,34,35]. One is a binding model, in which the interaction of the denaturant with the protein can be treated as specific binding [3,36]. And another is a solvent-exchange model, in which the interactions of both the solvent (water) and co-solvent (urea) with the protein are treated explicitly in an expression that involves the interchange between both components at a particular interaction 'site' on the protein [37].

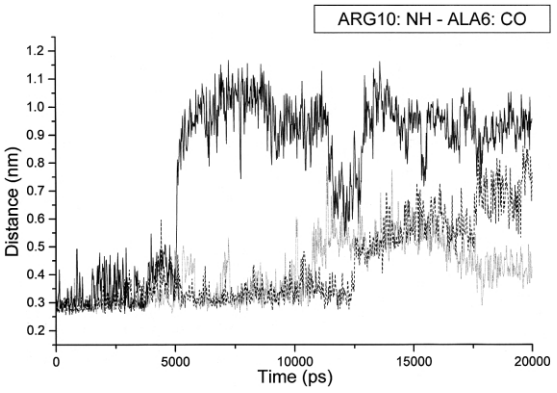

Fig. 7. Distances (nm) between ARG10-NH and ALA6-CO group as a function of time for all three simulations (dot-CW, dash-CU and solid-HW). When the distances are beyond 0.35 nm, the hydrogen bonds were broken.

Table 2
Hydrogen-bonding interactions between solvent molecules (urea or water) and amide unit (NH and CO group) of ARG10

ST(ns)	Number of H-bonds[a] (average residence time: ps)					
	CW		CU			
	Water		Water		Urea	
	(AA)NH[b]	(AA)CO[c]	(AA)NH	(AA)CO	(AA)NH	(AA)CO
1	3 (5)[d]	126 (11)	1 (5)	26 (35)	1 (10)	16 (56)
2	1 (5)	191 (10)	3 (13)	10 (59)	1 (105)	13 (100)
3	0 (0)	178 (10)	4 (21)	16 (31)	1 (110)	24 (52)
4	1 (5)	187 (10)	1 (10)	5 (65)	1 (5)	14 (111)
5	2 (10)	151 (11)	0 (0)	24 (44)	0 (0)	15 (60)
6	6 (96)	124 (11)	0 (0)	22 (23)	0 (0)	31 (50)
7	6 (12)	138 (10)	0 (0)	14 (23)	1 (20)	31 (52)
8	2 (115)	164 (10)	0 (0)	14 (32)	1 (5)	24 (61)
9	3 (5)	197 (11)	0 (0)	20 (31)	1 (5)	22 (54)
10	4 (6)	201 (10)	1 (5)	29 (24)	0 (0)	20 (61)
11	1 (135)	212 (9)	2 (13)	37 (25)	0 (0)	26 (40)
12	47 (20)	209 (10)	2 (5)	23 (17)	1 (5)	22 (73)
13	62 (17)	195 (10)	1 (5)	50 (23)	1 (505)	22 (23)
14	55 (18)	199 (10)	2 (10)	18 (27)	1 (960)	23 (74)
15	58 (18)	189 (10)	0 (0)	12 (12)	1 (735)	11 (178)
16	57 (19)	198 (9)	0 (0)	15 (23)	0 (0)	22 (73)
17	64 (16)	192 (10)	0 (0)	34 (21)	0 (0)	30 (52)
18	50 (13)	201 (9)	0 (0)	15 (28)	0 (0)	26 (65)
19	49 (16)	194 (9)	1 (5)	19 (18)	1 (900)	27 (71)
20	61 (17)	200 (10)	2 (5)	19 (26)	1 (975)	26 (56)

[a] The same criterion of hydrogen bonds was used as Table 1.
[b] Hydrogen bonds between solvent molecules and NH group of the residue.
[c] Hydrogen bonds between solvent molecules and CO group of the residue.
[d] Hydrogen bonds that are found within each 1 ns simulation are listed and the average residence times of these hydrogen bonds are in parentheses.

Table 3
Multiple hydrogen bonds[a] formed between 94urea, 113urea and residues (10ARG, 13MET and 15SER)

Urea	Residues	Residence time (ps)	T_b (ps)[b]	T_e (ps)[c]
94urea(O_2)[d]	10ARG(NH)	2190	12485	14760
94urea(N_3H_4)	15SER(O_1)	2190	12000	14990
94urea(N_3H_4)	15SER(O_2)	1065	12110	14720
94urea(N_6H_7)	15SER(O_2)	2145	12000	14775
94urea(N_6H_8)	15SER(O_1)	1160	12000	14775
94urea(N_6H_8)	13MET(O)	1420	12035	14770
113urea(O_2)	10ARG(NH)	1870	18045	20000
113urea(N_3H_4)	15SER(O_2)	830	18015	19985
113urea(N_3H_4)	15SER(O_1)	1645	18145	20000
113urea(N_6H_7)	15SER(O_2)	1510	18005	20000
113urea(N_6H_7)	15SER(O_1)	1050	18020	20000
113urea(N_6H_8)	13MET(O)	1095	18180	19900

[a] The same criterion of hydrogen bond was used as Table 1.
[b] T_b: the first time when the hydrogen bond was found during the simulation.
[c] T_e: the last time when the hydrogen bonds was found during the simulation.
[d] The groups that are involved in hydrogen bonds are in parentheses.

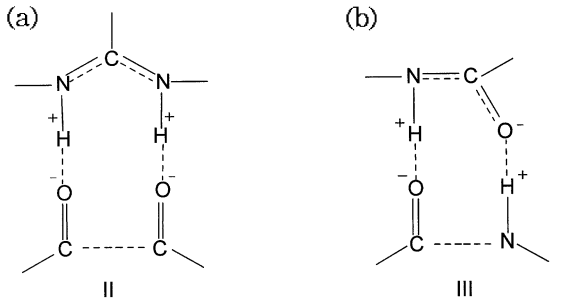

Fig. 8. Two possible forms of multiple hydrogen bonds between urea and amide units on the peptide [33]. (a) Structure II and (b) structure III.

Table 4 shows the binding sites that are involved in hydrogen bonds with water and urea molecules. The data suggest that the binding sites, which can form hydrogen bonds with urea or water molecules, are almost the same, that is, the solvent exchange model is physically reasonable. Schellman and Gassner found that experimental data can be fitted reasonably well with either the binding model or the solvent exchange model; fitting the data did not distinguish between these two models [38]. Since urea can form more hydrogen bonds than water does and the $\tau_{1/2}$ of urea-protein hydrogen bonds is larger than that of water-protein hydrogen bonds (average 8.099 ps and 2.248 ps, respectively), the binding model may be a good approximation of the experiment's data.

3.4. Comparison between urea and thermal-induced denaturation

3.4.1. Cluster analysis

Structures of the peptide were extracted from the trajectories at 5 ps intervals (a total of 4001 structures per simulation) for cluster analysis (see Section 2). Clusters with more than 20 member structures (more than 0.5% of the ensemble of all 4001 structures) are listed in Table 5 for each of the three simulations. In the simulation of CW, a total of 21 clusters were found, of which 13 contained more than 20 member structures. The backbone atom-positional RMSD (residues 4–8) between the central structure of a cluster and the initial structure, are from 0.0160 to 0.0633 nm. In CU, a total of 9 clusters were found, of which 6 contained more than 20 members. The RMSD are from 0.0153 to 0.0893 nm. A total of 177 clusters were found in HW, of which 47 contained more than 20 members. The RMSD are from 0.0157 to 0.3136 nm. The number of clusters in CU is less than the case of CW and HW, which indicates urea's stabilization effect on the partly unfolded form of the peptide.

3.4.2. Essential dynamics analysis

Essential dynamics analyses (see Section 2) were performed on 0.2–20 ns for all three simulations. A least-squares translational and rotational fit was performed for all frames in the chosen time relative to the initial structure using the heavy atoms of residues 4–8. The covariance ma-

Table 4
The number of 'binding sites' on the peptide that are involved in hydrogen bonds[a] with urea or water molecules

ST (ns)	Binding sites			
	CW	CU		HW
	pr[b]-h	pr-h[c]	pr-u[d]	pr-h
1	50	50	48	52
2	51	47	49	50
3	52	47	49	51
4	51	49	49	53
5	50	45	47	50
6	51	44	46	52
7	51	44	49	53
8	53	43	47	53
9	51	41	47	53
10	49	44	48	52
11	53	45	46	53
12	51	49	47	53
13	50	48	47	52
14	51	46	45	53
15	51	42	46	53
16	49	44	46	53
17	49	44	47	53
18	51	44	47	53
19	51	44	46	53
20	52	48	47	52

[a] The same criterion of hydrogen bonds was used as Table 1.
[b] Protein.
[c] Water.
[d] Urea.

Table 5
Clusters with more than 20 member structures for all three simulations

Cluster	CW		CU		HW	
	RMSD[a] (nm)	Members[b]	RMSD (nm)	Members	RMSD (nm)	Members
1	0.0242	1251	0.0893	2652	0.1734	361
2	0.0406	778	0.0452	566	0.0765	239
3	0.0571	575	0.0522	384	0.2377	201
4	0.0356	406	0.0813	323	0.2150	177
5	0.0180	221	0.0153	31	0.0309	175
6	0.0297	162	0.0807	25	0.0295	170
7	0.0174	152			0.0157	144
8	0.0633	116			0.1449	118
9	0.0160	111			0.2178	109
10	0.0191	53			0.1288	107
11	0.0631	51			0.2169	99
12	0.0493	47			0.1296	93
13	0.0514	45			0.1209	83
14					0.1668	83
15					0.0826	70
16					0.1059	70
17					0.2247	64
18					0.2036	64
19					0.1847	55
20					0.1666	54
21					0.2559	54
22					0.1561	53
23					0.1548	46
24					0.1166	42
25					0.1550	36
26					0.2213	33
27					0.2193	32
28					0.2784	30
29					0.1745	29
30					0.2375	29
31					0.2279	29
32					0.0246	28
33					0.1649	28
34					0.1612	27
35					0.2567	27
36					0.1291	26
37					0.2033	26
38					0.1550	25
39					0.2258	25
40					0.0927	24
41					0.0802	24
42					0.2268	24
43					0.0517	23
44					0.1863	21
45					0.3136	21
46					0.2146	20
47					0.0316	20

[a] The backbone atom-positional RMSD (residues 4–8) between the central structures of the cluster and the initial structure.
[b] The number of member structures in the cluster are shown.

trix of the positional deviations is constructed using the coordinates of all heavy atoms in residues 4–8 (the dimension of the matrix is 105 × 105). It is clear from Fig. 9 that even for a small peptide the configurational space is not homogeneous. Most of the significant motions reside in a limited subset of the first few eigenvectors. In CW, only the first and third eigenvectors (e_1^{CW} and e_3^{CW}) are essential (see materials and methods). In CU, eigenvectors 1, 2, 3 and 7 (e_1^{CU}, e_2^{CU}, e_3^{CU} and e_7^{CU}) and in HW, eigenvectors 1, 2, 3, 4 and 5 (e_1^{HW}, e_2^{HW}, e_3^{HW}, e_4^{HW} and e_5^{HW}) are essential.

CU and HW contain more essential motions, which can be ascribed to the denaturant conditions. Table 6 lists eigenvalues of essential modes, as well as minimal and maximal projections of trajectory along these modes. In CW, most of the 'native motions' of the peptide reside in e_1^{CW}. According to the time where the frame in the trajectory has the minimal and maximal projections, respectively, the motions along e_1^{CU} are essentially the 'native motions' and most of the unfolding motions seem to limit in the subset of e_2^{CU}. The same analyses to HW reveal that, most of the essential modes (e_1^{HW}, e_2^{HW}, e_3^{HW} and e_5^{HW}) of HW are related neither to the 'native motions' nor to the unfolding motions, just fluctuations after unfolding. Only e_4^{HW} may relate to the unfolding motions. We calculate inner products of eigenvector sets of different simulations further (Table 7) (see Section 2), which show agreement with the results in Table 6. The inner product between e_1^{CW} and e_1^{CU} is high — 0.729 (Table 7a), which indicates a dynamical similarity between two modes. The inner products of e_2^{CU} and e_4^{HW}

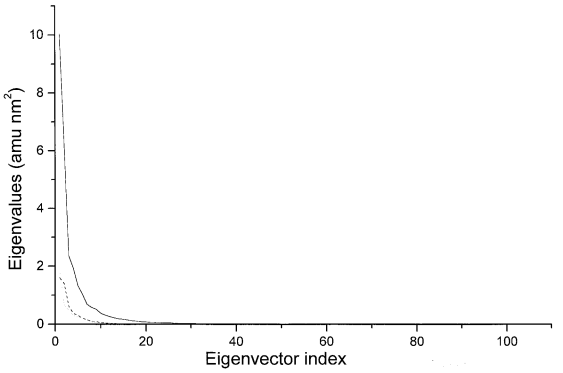

Fig. 9. Eigenvalues in decreasing order of magnitude, obtained by diagonalizing 0.2–20 ns of CW (dot), CU (dash) and HW (solid) covariance matrix (heavy atoms of residues 4–8 only).

Table 6
Eigenvalues of essential modes and projection of trajectory along these modes

Eigenvector[a]	Eigenvalue (amu nm^2)	Projection$_{min}$ (amu$^{1/2}$nm)[b]		Projection$_{max}$ (amu$^{1/2}$nm)[c]	
		Value	Time (ps)	Value	Time (ps)
e_1^{CW}	**1.819**[d]	**−2.031**	**4860**	**3.718**	**8080**
e_3^{CW}	0.469	−1.940	11400	2.064	15580
e_1^{CU}	1.604	−2.104	1120	2.436	340
e_2^{CU}	**1.397**	**−4.099**	**820**	**1.813**	**14280**
e_3^{CU}	0.625	−2.809	15340	2.072	7300
e_7^{CU}	0.157	−4.222	15020	0.464	1240
e_1^{HW}	10.391	−7.071	15160	7.410	13540
e_2^{HW}	6.136	−6.326	19400	3.119	19300
e_3^{HW}	2.362	−3.382	13100	7.002	11820
e_4^{HW}	**1.926**	**−5.354**	**2520**	**4.162**	**18220**
e_5^{HW}	1.331	−3.540	19940	5.189	12620

[a] e_i^{CW} (i = 1, 3)-essential modes of CW. e_i^{CU} (i = 1, 2, 3 and 7)-essential modes of CU. e_i^{HW} (i = 1, 2, 3, 4 and 5)-essential modes of HW.

[b] The frame in the trajectory that has the minimal projection along the eigenvector.

[c] The frame in the trajectory that has the maximal projection along the eigenvector.

[d] The most important values are marked in bold.

Table 7
Inner products of eigenvectors between essential modes from different simulations

A[a]	e_1^{CU}	e_2^{CU}	e_3^{CU}	e_7^{CU}	
e_1^{CW}	**0.729**[b]	**0.004**	0.030	0.000	
e_3^{CW}	0.002	0.217	0.122	0.289	
B[c]	e_1^{HW}	e_2^{HW}	e_3^{HW}	e_4^{HW}	e_5^{HW}
e_1^{CW}	0.002	0.176	0.218	**0.007**	0.409
e_3^{CW}	0.034	0.003	0.012	0.011	0.058
C[d]	e_1^{HW}	e_2^{HW}	e_3^{HW}	e_4^{HW}	e_5^{HW}
e_1^{CU}	0.050	0.015	0.198	0.001	0.365
e_2^{CU}	0.307	0.008	0.079	**0.009**	0.036
e_3^{CU}	0.192	0.074	0.031	0.071	0.013
e_7^{CU}	0.016	0.006	0.016	0.021	0.073

[a] Between CW (e_i^{CW}) and CU (e_i^{CU}).
[b] The most important overlaps are marked in bold.
[c] Between CW (e_i^{CW}) and HW (e_i^{HW}).
[d] Between CU (e_i^{CU}) and HW (e_i^{HW}).

with e_1^{CW} are 0.004 and 0.007, respectively (Table 7a,b). These two modes are related not to the 'native motions', but to the unfolding motions. It should be noted that the inner product of e_4^{HW} with e_2^{CU} is low — 0.009 (Table 7c), which suggests that the essential modes of urea and thermal-induced unfolding are different.

Atomic displacements corresponding to one eigenvector represent the contribution of the atom's motion along the eigenvector (Fig. 10). The heavy atoms' displacements of Ala4, Ala5 and Ala6 are low along e_1^{CW} (Fig. 10a), which is consistent with the high helix-forming potential of Ala [27,28]. But the same values along e_2^{CU} (Fig. 10b) and e_4^{HW} (Fig. 10c) are relatively high, which may lead to the break of the α-helix. It is clearly seen that atomic displacements along e_2^{CU} and e_4^{HW} show many differences (Fig. 10b,c). In Fig. 11, 3D representations of the motions along some essential modes (e_1^{CW}, e_2^{CU} and e_4^{HW}) are shown, respectively.

4. Conclusion

Molecular dynamics simulations of the S-peptide analogue at different conditions (CW, CU, HW) showed that the α-helix of the peptide is relatively stable at low temperature (less than 278 K) in water solution, while at high temperature (358 K) or in urea solution, the peptide loses its native α-helix.

The analysis of interactions between urea and the peptide reveal some aspects of the mechanism of urea-induced denaturation: (1) urea molecules interact more favorably with nonpolar groups of the protein than water does and can

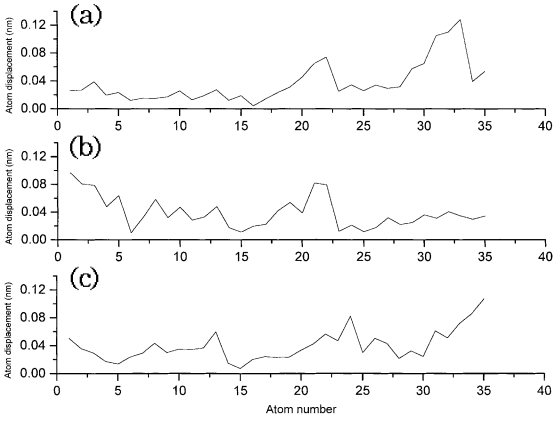

Fig. 10. Atom displacements along some eigenvectors. (a) The first eigenvector of CW (e_1^{CW}), (b) the second eigenvector of CU (e_2^{CU}) and (c) the fourth eigenvector of HW (e_4^{HW}).

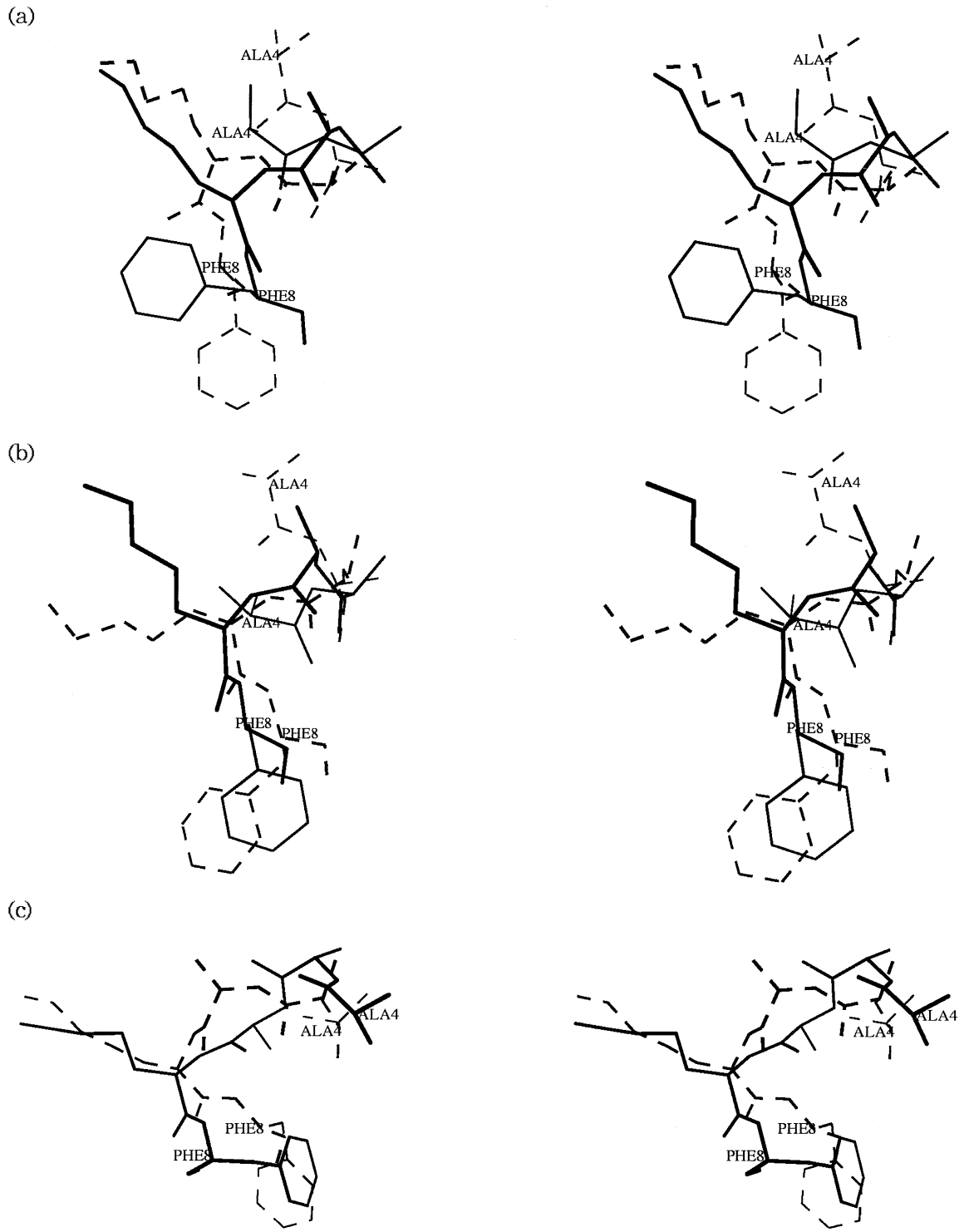

Fig. 11. Stereo views of two configurations obtained by projecting the heavy atoms' motions of residues 4–8 onto the eigenvector. (a) The first eigenvector of CW (e_1^{CW}), (b) The second eigenvector of CU (e_2^{CU}) and (c) The fourth eigenvector of HW (e_4^{HW}). The two extreme structures (dot and solid) along this eigenvector are shown. The pictures are created using the program Molscript [39].

diminish the hydrophobic effect; and (2) urea can form stable multiple hydrogen bonds with the amide units on the peptide and break native hydrogen bonds.

Compared to HW, the result of cluster analysis and the essential modes of unfolding in the simulation of CU are different. These results may suggest some differences between urea and thermal-induced denaturation.

Acknowledgements

We gratefully thank Prof. H.J.C. Berendsen for providing us with the GROMACS programs. We also gratefully thank Mr B. Hess and Mr B.L. de Groot for their useful advises. Mr J. Zhu in our group has provided us with useful algorithms. This work was supported by the Chinese National Fundamental Research Project, Grant No. G1999075605 and the Chinese National Natural Science Foundation, Grant No. 399906000.

References

[1] C. Tanford, Protein denaturation C. Theoretical models for the mechanism of denaturation, Adv. Protein Chem. 24 (1970) 1–95.
[2] J.A. Schellman, Solvent denaturation, Biopolymers 17 (1978) 1305–1322.
[3] J.A. Schellman, Selective binding and solvent denaturation, Biopolymers 26 (1987) 549–559.
[4] J.A. Schellman, The thermodynamic stability of proteins, Annu. Rev. Biophys. Chem. 16 (1987) 115–137.
[5] T.E. Creighton, Stability of folded conformations, Curr. Opin. Struct. Biol. 1 (1991) 5–16.
[6] M. Roseman, W.P. Jencks, Interaction of urea and other polar compounds in water, J. Am. Chem. Soc. 97 (1975) 631–640.
[7] R. Breslow, T. Guo, Surface tension measurements show that chaotropic salting-in denaturants are not just water-structure breakers, Proc. Natl. Acad. Sci. USA 87 (1) (1990) 167–169.
[8] G.I. Makhatadze, P.L. Privalov, Protein interaction with urea and guanidinium chloride: a calorimetric study, J. Mol. Biol. 226 (2) (1992) 491–505.
[9] J.W. Wu, Z.X. Wang, New evidence for the denaturant binding model, Protein Sci. 8 (10) (1999) 2090–2097.
[10] Q. Zou, S.M. Habermann-Rottinghaus, K.P. Murphy, Urea effects on protein stability: hydrogen bonding and the hydrophobic effects, Proteins Struct. Funct. Genet. 31 (1998) 107–115.
[11] J. Tirado-Rives, M. Oroczo, W.L. Jorgenson, Molecular dynamics simulations of the unfolding of barnase in water and 8 M aqueous urea, Biochemistry 36 (1997) 7313–7329.
[12] A. Caflisch, M. Karplus, Structural details of urea binding to barnase: a molecular dynamics analysis, Structure Fold. Des. 7 (5) (1999) 477–488.
[13] J. Tirado-Rives, W.L. Jorgensen, Molecular dynamics simulations of an α-helical analogue of Ribonuclease A S-peptide in water, Biochemistry 30 (1991) 3864–3871.
[14] W.A. Klee, Studies on the conformation of Ribonuclease S-peptide, Biochemistry 7 (8) (1968) 2731–2736.
[15] F.C. Bernstein, T.F. Koetzle, G.J.B. Williams, E.F. Meyer, M.D. Brice Jr., J.R. Rodgers, O. Kennard, T. Shimanouchi, M. Tasumi, The protein databank: a computer-based archival file for macromolecular structures, J. Mol. Biol. 112 (3) (1977) 535–542.
[16] H.J.C. Berendsen, J.P.M. Postma, W.F. Van Gunsteren, A.Di. Nola, J.R. Haak, Molecular dynamics with coupling to an external bath, J. Chem. Phys. 81 (1984) 3684–3690.
[17] W.F. Van Gunsteren, H.J.C. Berensen, Gromos-87 manual, Biomos BV, The Netherlands, 1987.
[18] D. Van der Spoel, A.R. Van Buuren, E. Apol, D.P. Tieleman, A.L.T.M. Sijbers, B. Hess, K.A. Feenstra, E. Lindahl, R. Van Drunen, H.J.C. Berendsen, Gromacs User Manual Version 2.0, Bioson Research Institute, The Netherlands, 1999.
[19] H.J.C. Berendsen, J.R. Grigera, T.P. Straatsma, The missing term in effective pair potentials, J. Phys. Chem. 91 (1987) 6269–6271.
[20] B. Hess, H. Bekker, H.J.C. Berendsen, J.G.E.M. Fraaije, LINCS: A linear constraint solver for molecular simulations, J. Comp. Chem. 18 (1997) 1463–1472.
[21] D. Van der Spoel, R. Van Drunen, H.J.C. Berendsen. Groningen Machine for chemical simulations, department of biophysical chemistry, Bioson Research Institute Nijenborgh 4 NL-9717 AG Groningen, 1999.
[22] W. Kabsch, C. Sander, Dictionary of protein secondary structure: pattern recognition of hydrogen-bonded and geometrical features, Biopolymers 22 (1983) 2576–2637.
[23] H.Y. Liu, Z.H. Duan, Q.M. Luo, Y.Y. Shi, Structure-based design by dynamically assembling molecular building blocks at binding site, Proteins Struct. Funct. Genet. 36 (1999) 462–470.
[24] A. Amadei, A.B.M. Linssen, H.J.C Berendsen, Essential dynamics of proteins, Proteins Struct. Funct. Genet. 17 (1993) 412–425.
[25] L.D. Creveld, A. Amadei, R.C. Van Schaik, H.A.M. Pepermans, J. de Vlieg, H.J.C. Berendsen, Identification of functional and unfolding motions of cutinase as obtained from molecular dynamics computer simulations, Proteins Struct. Funct. Genet. 33 (1998) 253–264.
[26] B.L. de Groot, D.M.F. Van Aalten, A. Amadei, H.J.C. Berensen, The consistency of large concerted motions in proteins in molecular dynamics simulations, Biophys. J71 (1996) 1707–1713.

[27] S. Marqusee, R.L. Baldwin, Helix stabilization by Glu − …Lys + salt bridges in short peptides of de nove design, Proc. Natl. Acad. Sci. USA 84 (1987) 8898–8902.
[28] S. Padmanabhan, S. Marqusee, T. Ridgeway, T.M. Laue, R.L. Baldwin, Relative helix-forming tendencies of nonpolar amino acids, Nature 344 (1990) 268–270.
[29] T.E. Creighton, Proteins-structures & molecular properties, (Medical Research Council), W.H. Freeman and Company, New York, 1984.
[30] J. Tsai, M. Gerstein, M. Levitt, Keeping the shape but changing the charge: a simulation of urea and its isosteric analogs, J. Chem. Phys. 104 (1996) 9417–9430.
[31] R.A. Kuharski, P.J. Rossky, Solvation of hydrophobic species in aqueous urea solution: a molecular dynamics study, J. Am. Chem. Soc. 106 (1984) 5794–5800.
[32] N. Muller, A model for the partial reversal of hydrophobic hydration by addition of a urea-like co-solvent, J. Phys. Chem. 94 (1990) 3856–3859.
[33] D.R. Robinson, W.P. Jencks, The effect of compounds of the urea-guanidinium class on the activity coefficient of acetyltetraglycine ethyl esters and related compounds, J. Am. Chem. Soc. 87 (1965) 2462–2470.
[34] J.A. Schellman, The thermodynamics of solvent exchange, Biopolymers 34 (8) (1994) 1015–1026.
[35] C.N. Pace, Determination and analysis of urea and guanidine hydrochloride denaturation curves, Methods Enzymol. 131 (1986) 266–280.
[36] K. Aune, C. Tanford, Thermodynamics of the denaturation of Lysozyme by guanidine hydrochloride II. Dependence on denaturant concentration at 25 degrees, Biochemistry 8 (11) (1969) 4586–4590.
[37] J.A. Schellman, A simple model for solvation in mixed solvents: applications to the stabilization and destabilization of macromolecular structures, Biophys. Chem. 37 (1990) 121–140.
[38] J.A. Schellman, N.C. Gassner, The enthalpy of transfer of unfolded protein into solutions of urea and guanidinium chloride, Biophys. Chem. 59 (1996) 259–275.
[39] P.J. Kraulis, MOLSCRIPT: a program to produce both detailed and schematic plots of protein structures, J. Appl. Crystallog 24 (1991) 946–950.